

Supporting Information

Construction of Fully π -Conjugated, Diyne-Linked Conjugated Microporous Polymers Based on Tetraphenylethene and Dibenzo[*g,p*]chrysene Units for Energy Storage

Mohamed Gamal Mohamed,^{*a,b,1} Santosh U. Sharma,^{c,1} Pei-Tzu Wang,^a Mervat Ibrahim,^d Meng-Hao Lin,^e Cheng-Liang Liu,^e Mohsin Ejaz,^a Hung-Ju Yen,^{*c} and Shiao-Wei Kuo^{*a,f}

^a *Department of Materials and Optoelectronic Science, College of Semiconductor and Advanced Technology Research, Center for Functional Polymers and Supramolecular Materials, National Sun Yat-Sen University, Kaohsiung 804, Taiwan.*

^b *Chemistry Department, Faculty of Science, Assiut University, Assiut 71515, Egypt.*

^c *Institute of Chemistry, Academia Sinica, Taipei 115, Taiwan.*

^d *Chemistry Department, Faculty of Science, New Valley University, El-Kharja, 72511, Egypt.*

^e *Department of Materials Science and Engineering, National Taiwan University, Taipei 10617, Taiwan.*

^f *Department of Medicinal and Applied Chemistry, Kaohsiung Medical University, Kaohsiung 807, Taiwan.*

Corresponding authors:

mgamal.eldin12@yahoo.com (M. G. Mohamed), hjyen@gate.sinica.edu.tw (H. J. Yen) and kuosw@faculty.nsysu.edu.tw (S. W. Kuo).

¹These authors equally contributed.

Characterization

FTIR spectra were collected on a Bruker Tensor 27 FTIR spectrophotometer with a resolution of 4 cm^{-1} by using the KBr disk method. ^{13}C nuclear magnetic resonance (NMR) spectra were examined by using an INOVA 500 instrument with CDCl_3 as the solvent and TMS as the external standard. Chemical shifts are reported in parts per million (ppm). The thermal stabilities of the samples were performed by using a TG Q-50 thermogravimetric analyzer under an N_2 atmosphere; the cured sample (ca. 5 mg) was put in a Pt cell with a heating rate of $20\text{ }^\circ\text{C min}^{-1}$ from 100 to $800\text{ }^\circ\text{C}$ under a N_2 flow rate of 60 mL min^{-1} . Solid-state ^{13}C NMR was measured by JEOL JNM-LA300 spectrometer and standard CPMAS probe at 75.577 MHz. Wide-angle X-ray diffraction (WAXD) patterns were measured by the wiggler beamline BL17A1 of the National Synchrotron Radiation Research Center (NSRRC), Taiwan. A triangular bent Si (111) single crystal was used to get a monochromated beam having a wavelength (λ) of 1.33 Å. The morphologies of the polymer samples were examined by Field emission scanning electron microscopy (FE-SEM; JEOL JSM7610F) and also by transmission electron microscope (TEM) using a JEOL-2100 instrument at an accelerating voltage of 200 kV. BET surface area and porosimetry measurements of samples (ca. 40–100 mg) were measured using BEL MasterTM/BEL simTM (v. 3.0.0). N_2 adsorption and desorption isotherms were generated through incremental exposure to ultrahigh-purity N_2 (up to ca. 1 atm) in a liquid N_2 (77 K) bath. Surface parameters were calculated using BET adsorption models in the instrument's software. The pore size of the prepared samples was determined by using nonlocal density functional theory (NLDFT).

Electrochemical Characterization: The electrochemical experiments were performed in a three-electrode cell using an Autolab potentiostat (PGSTAT204) and 1 M KOH as the aqueous electrolyte. The GCE was used as the working electrode (diameter: 5.61 mm; 0.2475 cm^2); a Pt

wire was used as the counter electrode; Hg/HgO (RE-1B, BAS) was the reference electrode. All reported potentials refer to the Hg/HgO potential. A slurry was prepared by dispersing TPE-Diyne CMP or TBN-Diyne CMP (2 mg), carbon black (2 mg), and Nafion (10 wt%) in a mixture of (EtOH/ H₂O) (200 μL: 800 μL) and then sonicating for 1 h. A portion of this slurry (10 μL) was pipetted onto the tip of the electrode, which was then dried in air for 30 min before use. The electrochemical performance was studied through CV at various sweep rates (5–200 mV s⁻¹) and through the GCD method in the potential range from 0 to -1.00 V (vs. Hg/HgO) at various current densities (0.5–20 A g⁻¹) in 1 M KOH as the aqueous electrolyte solution.

The specific capacitance was calculated from the GCD data using the equation.

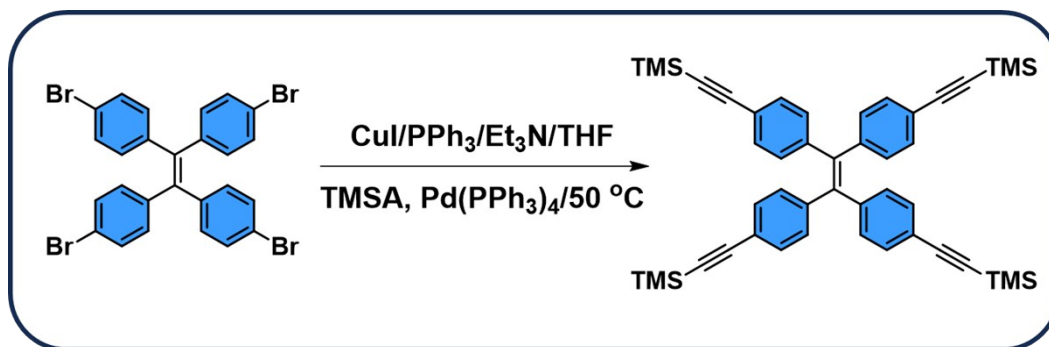
$$C_s = (I\Delta t)/(m\Delta V)$$

Where C_s (F g⁻¹) is the specific capacitance of the supercapacitor, I (A) is the discharge current, ΔV (V) is the potential window, Δt (s) is the discharge time, and m (g) is the mass of the NPC on the electrode. The energy density (E , W h kg⁻¹) and power density (P , W kg⁻¹) were calculated using the equations.

$$E = 1000C(\Delta V)^2/(2 \times 3600)$$

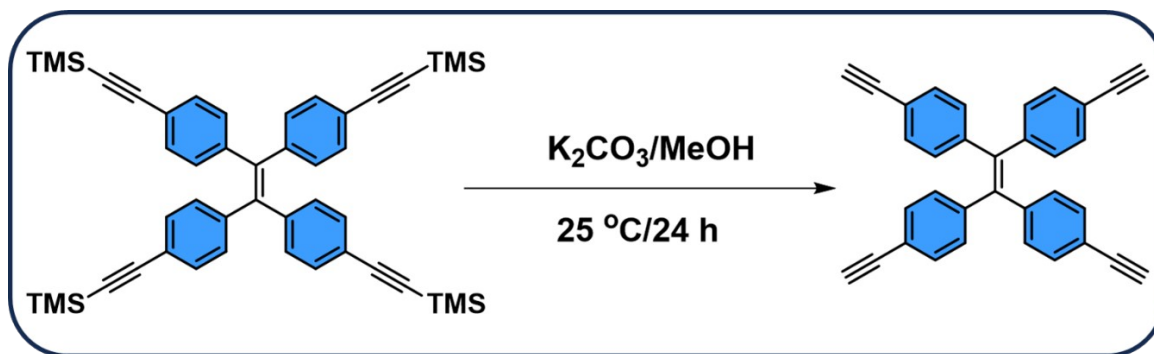
$$P = E/(t/3600)$$

Synthesis of 1,1,2,2-Tetrakis(4-((trimethylsilyl)ethynyl)phenyl)ethane (TPE-TMS)



A mixture of tetrakis(4-bromophenyl)ethylene (1.00 g, 1.54 mmol), CuI (0.0470 g, 0.240 mmol), PPh₃ (0.100 g, 0.380 mmol), and Pd(PPh₃)₄ (0.0860 g, 0.120 mmol) in THF (14 mL) and Et₃N (14 mL) was stirred in a two-neck flask at 50 °C for 30 min. Ethynyltrimethylsilane (TMSA, 1.21 g, 12.3 mmol) was added dropwise and then the mixture was heated under reflux at 50 °C for 3 days. The resulting mixture was filtered and concentrated. The residue was purified through flash chromatography (SiO₂; DCM) to give a white powder (0.75 g, 75%). FTIR (KBr, cm⁻¹): 3060 (aromatic C–H stretching), 2920 (aliphatic C–H stretching), 2155 (C≡C stretching), 1618 (C=C stretching). ¹H NMR (500 MHz, CDCl₃, δ, ppm): 7.24 (d, *J* = 8.4 Hz, 8H), 6.88 (d, *J* = 8.4 Hz, 8H), 0.22 (s, 36H, CH₃). ¹³C NMR (125 MHz, CDCl₃, δ, ppm): 144, 141, 132.7, 132, 122.3, 105.6, 95.8, 0.07.

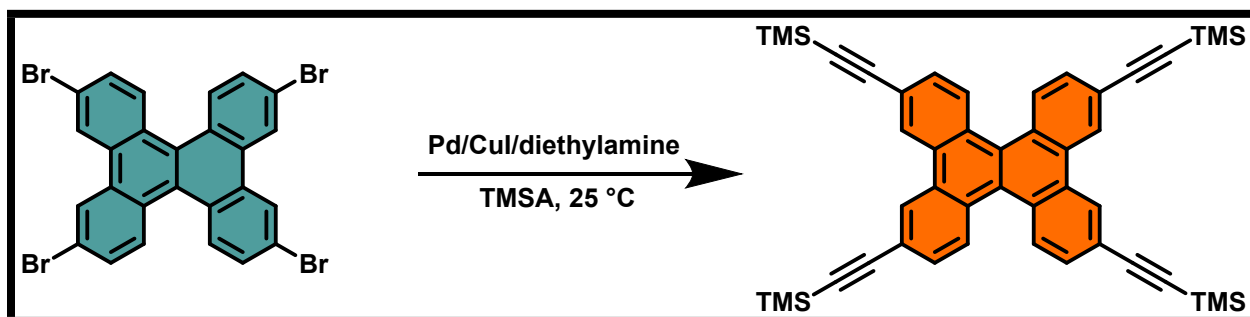
Synthesis of 1,1,2,2-Tetrakis(4-ethynylphenyl)ethene (TPE-TB)



Scheme S1. Synthesis of TPE-TB.

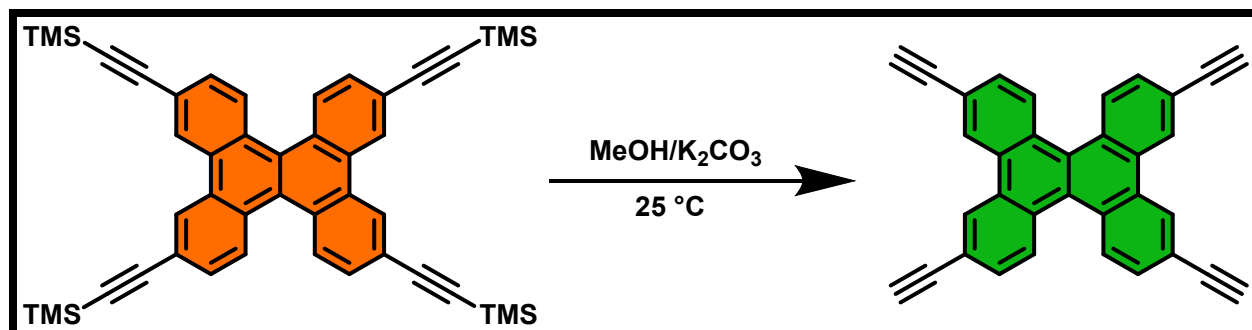
A mixture of K_2CO_3 (2 g, 14.48 mmol) and TPE-TMS (0.97 g, 1.44 mmol) in 25 mL of methanol was stirred at room temperature overnight. A pale-yellow precipitate [0.82 g] was obtained after filtration and drying. FTIR (**Figure S1**): 3273, 3042, 2109 ($C\equiv C$ unit). 1H NMR (500 MHz, $CDCl_3$, δ , ppm, **Figure S2**): 7.24-6.93 (16H, $H_b + H_c$), 3.06 (s, 4H, $\equiv C-H$, H_a). ^{13}C NMR (125 MHz, $CDCl_3$, δ , ppm, **Figure S3**): 143.8-121.24, 83.6 ($\equiv C-Ar$), 77.88 ($\equiv C-H$).

Synthesis of 2,7,10,15-tetrakis((trimethylsilyl)ethynyl)dibenzo[*g,p*]chrysene (TBN-TMS)



In 125 mL of diethylamine, 1.5 g of 2,7,10,15-tetrabromodibenzo[*g,p*]chrysene (2.33 mmol) was dissolved. Then the solution was treated with a combination of CuI (0.11 g), $Pd(PPh_3)_4$ (0.08 g), and ethynyltrimethylsilane (TMSA, 1.83 g, 18.63 mmol). After 24 h of stirring at 80 °C, the solvent was removed under reduced pressure, and the product was then purified using flash chromatography on a silica gel column with DCM as an eluent to produce a yellow solid (1.3 g, 86%). FTIR (KBr, cm^{-1}): 3291 ($C\equiv C-H$ stretching), 3031 (aromatic C-H stretching), 2957 (aliphatic C-H stretching), 2156 ($C\equiv C$ stretching), 1632 ($C=C$ stretching). 1H NMR (500 MHz, $CDCl_3$): δ 8.77, 8.47, 7.69, 0.34 (s, 36H, CH_3). ^{13}C NMR (125 MHz, $CDCl_3$, δ , ppm): 131.24, 128.74, 121.90, 105.38, 96.34, 30.59, 3.5.

Synthesis of 2,7,10,15-tetraethynyldibenzo[*g,p*]chrysene (TBN-TB)



Scheme S2. Synthesis of TBN-TB.

A mixture of K₂CO₃ (5 g, 36.17 mmol) and TBN-TMS (4.17 g, 5.83 mmol) in methanol/DCM (250 mL:170 mL) was stirred at room temperature overnight. Upon filtration, extraction, and drying, TBN-TB as an orange solid was obtained [3.34 g]. FTIR (**Figure S4**): 2106 (C≡C unit). ¹H NMR (500 MHz, CDCl₃, δ, ppm, **Figure S5**): 8.81-7.73 (12 H), 3.30 (s, 4H, ≡C-H, H_a). ¹³C NMR (125 MHz, CDCl₃, δ, ppm, **Figure S6**): 135.70-78.87 ppm.

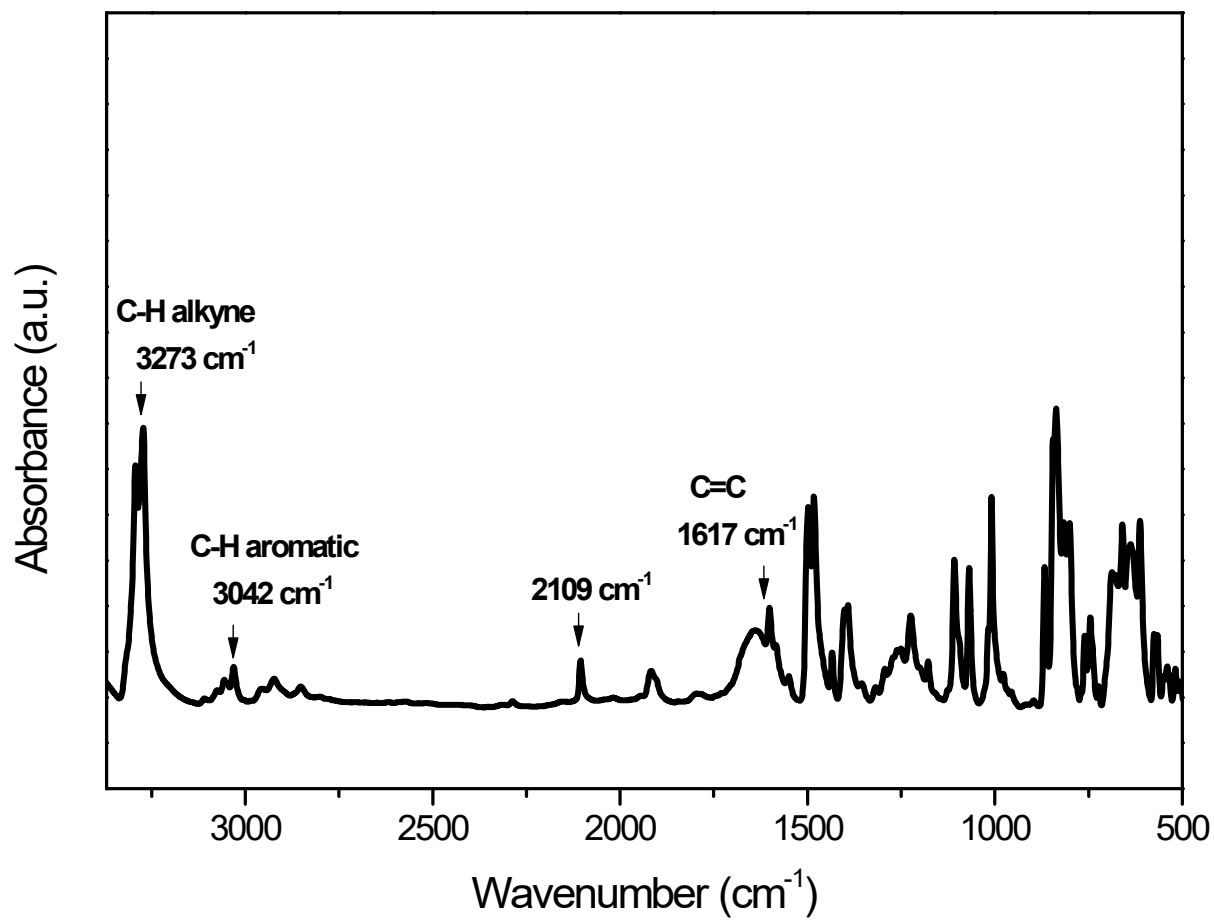


Figure S1. FT-IR spectrum of TPE-TB.

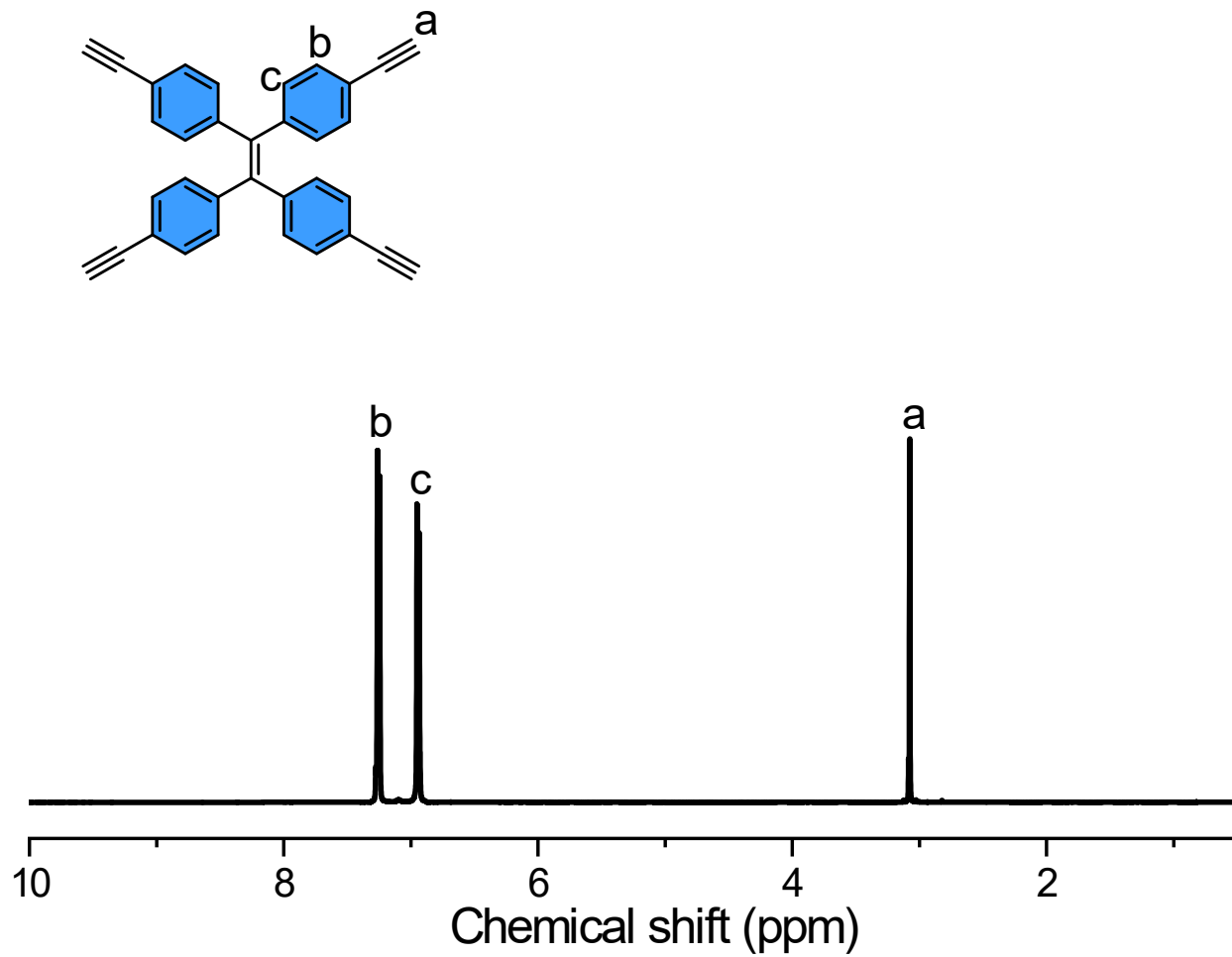


Figure S2. ^1H NMR spectrum of TPE-TB in CDCl_3 .

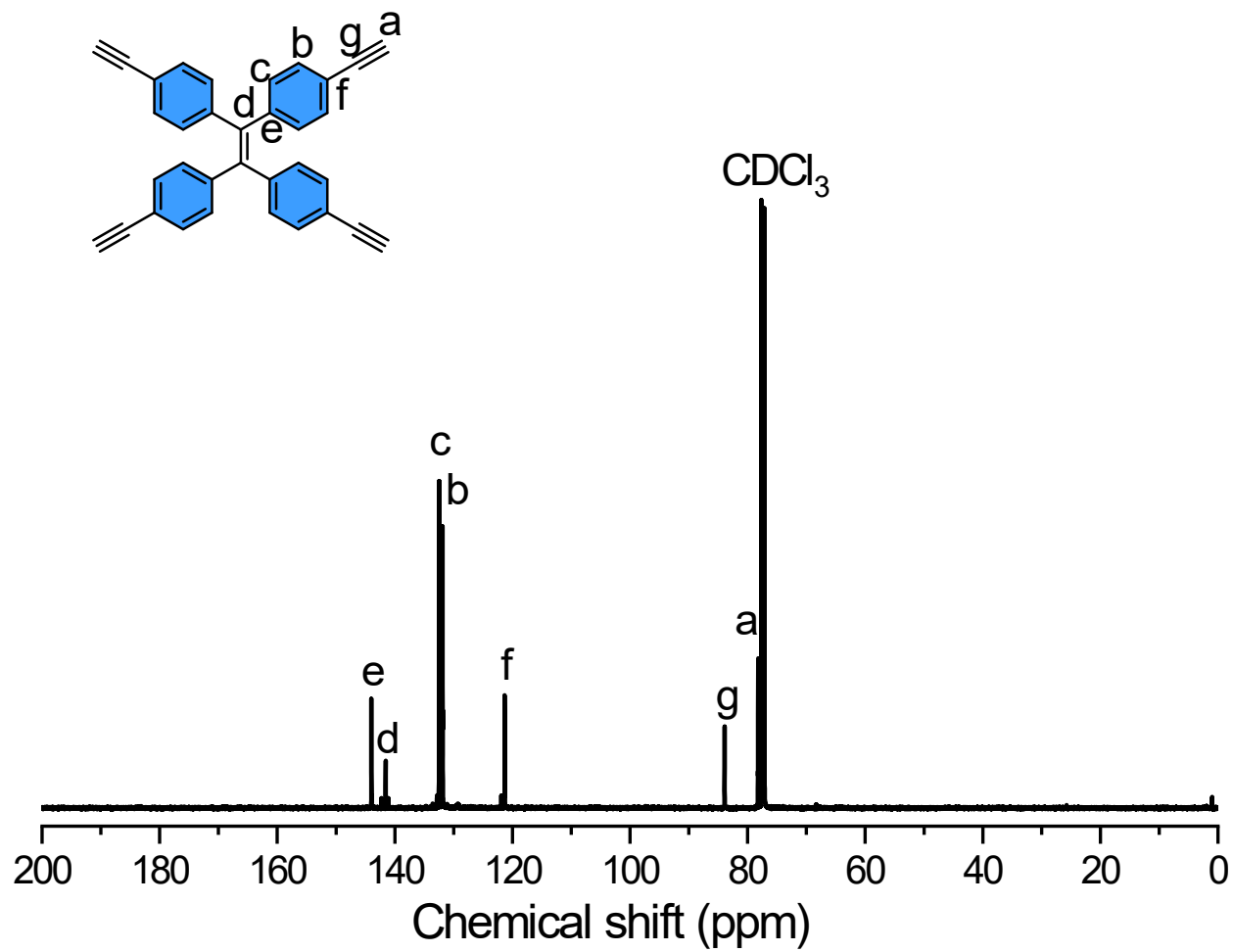


Figure S3. ¹³C NMR spectrum of TPE-TB in CDCl₃.

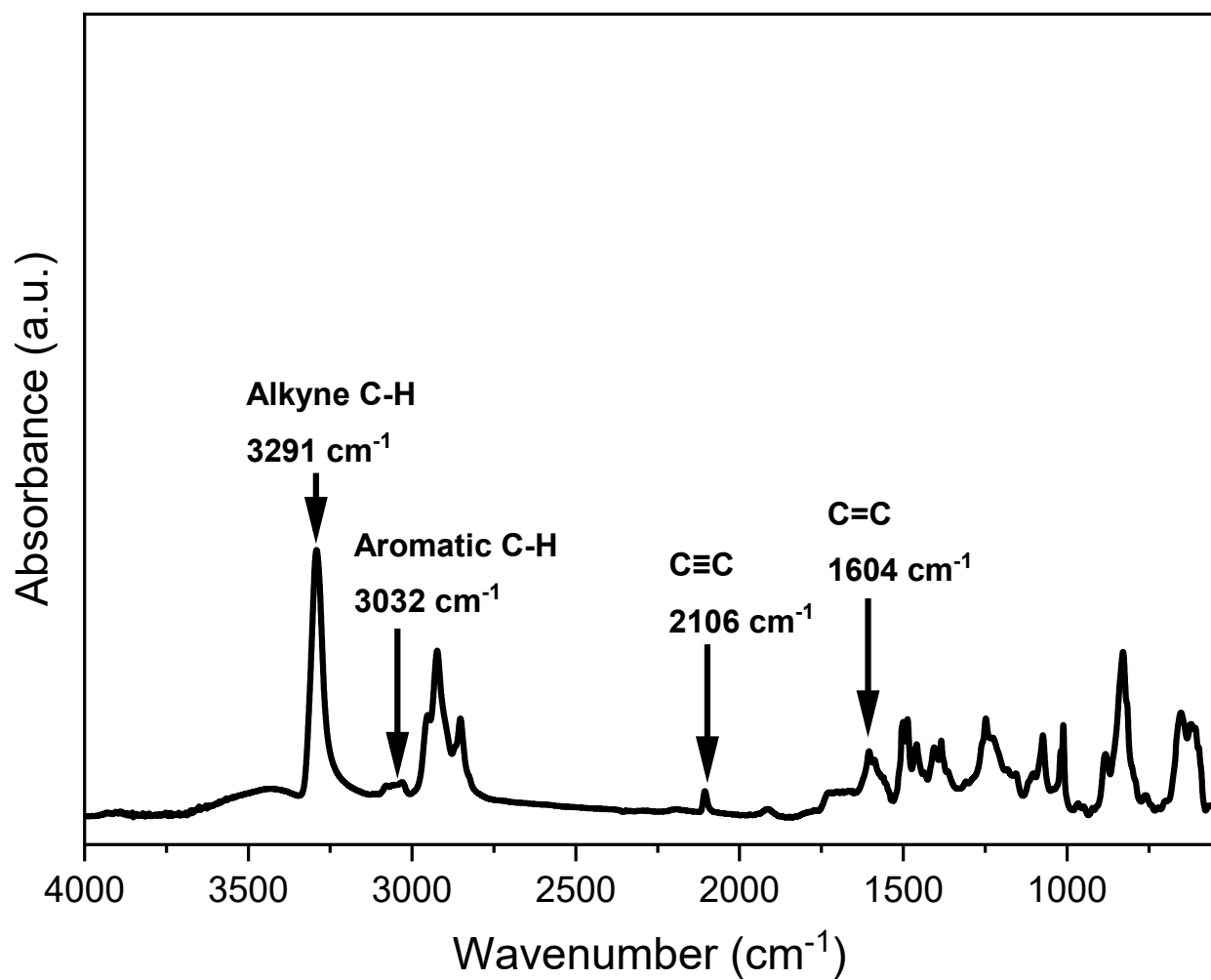


Figure S4. FTIR spectrum of TBN-TB.

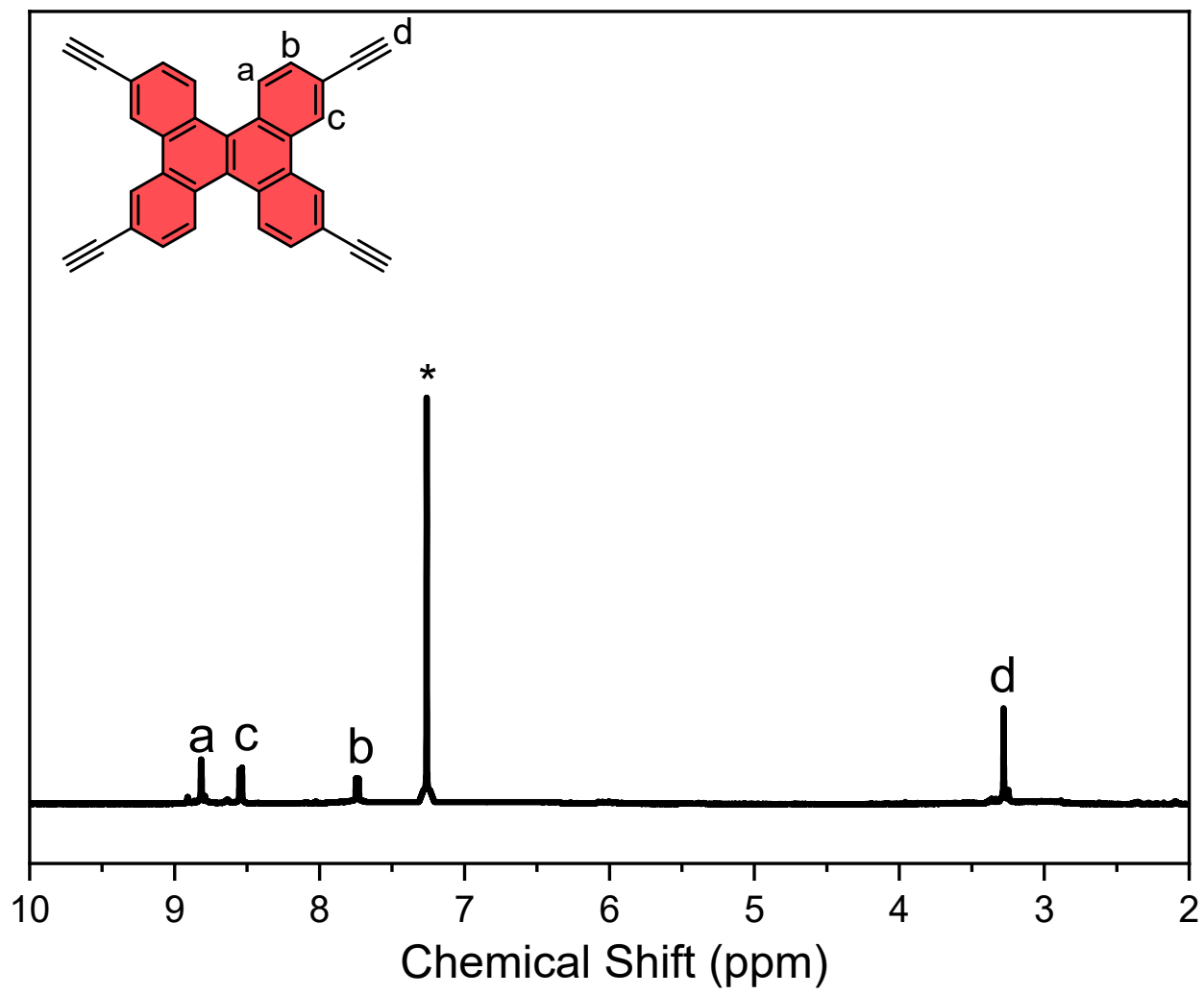


Figure S5. ^1H NMR spectrum of TBN-TB in CDCl_3 .

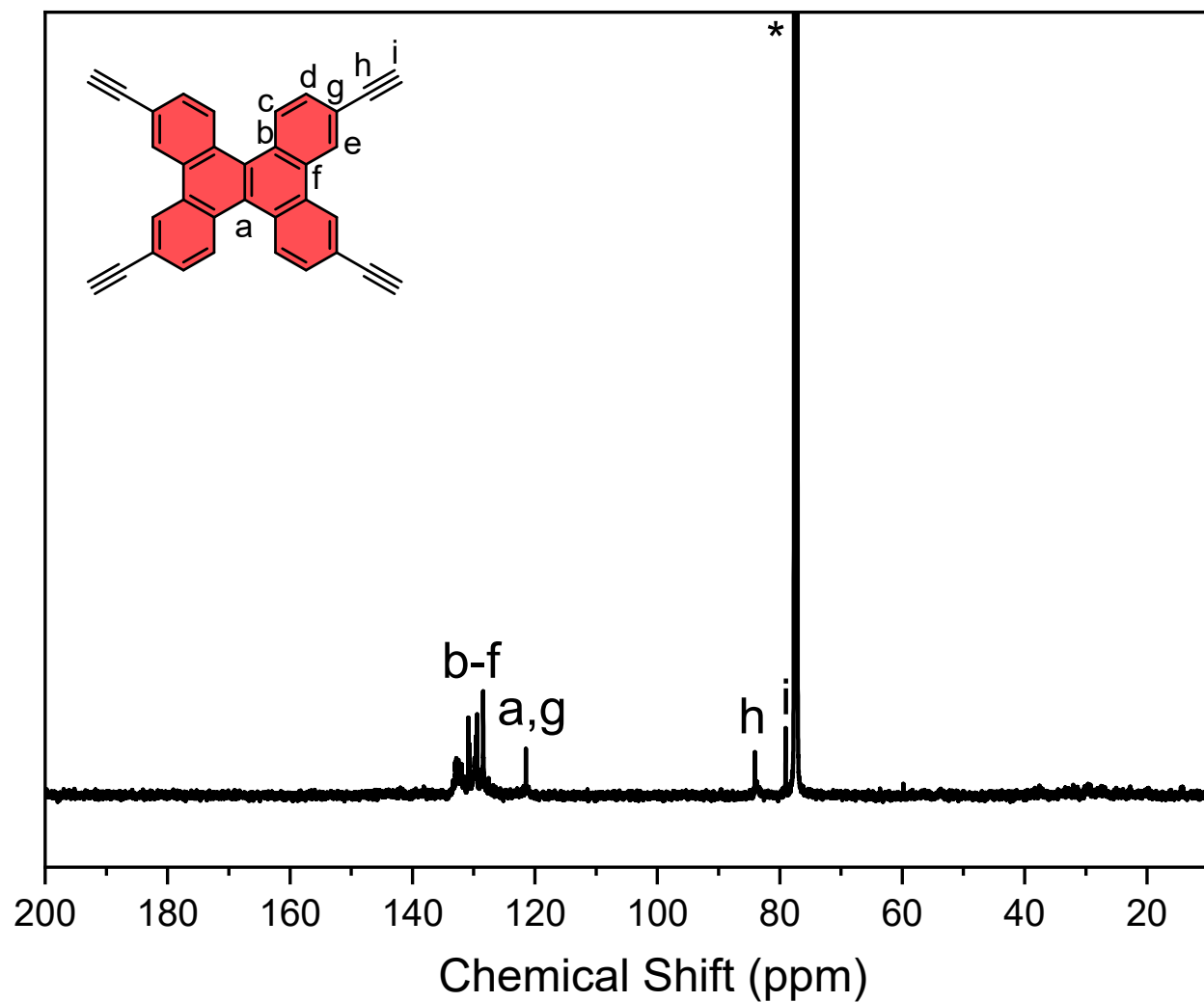


Figure S6. ^{13}C NMR spectrum of TBN-TB in CDCl_3 .

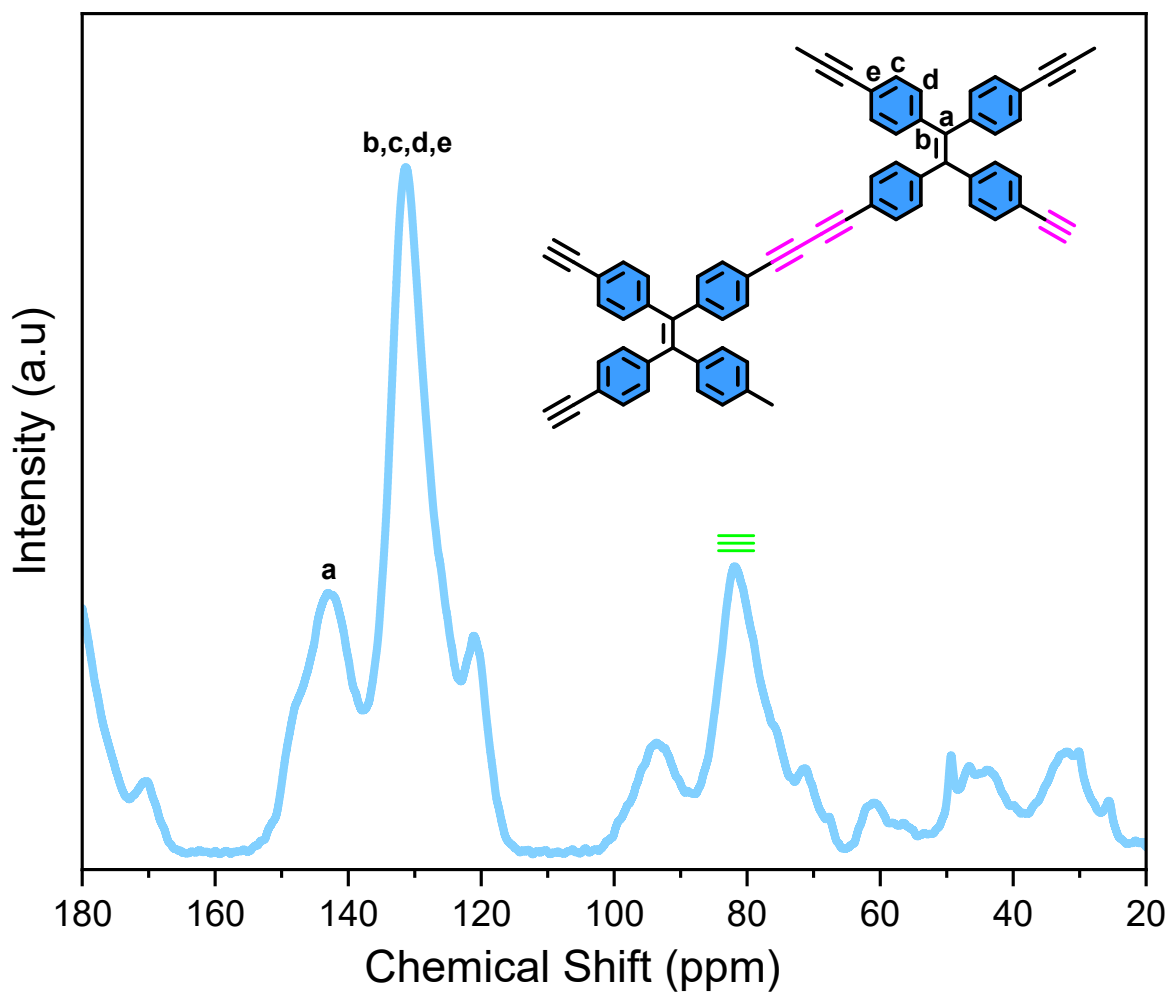
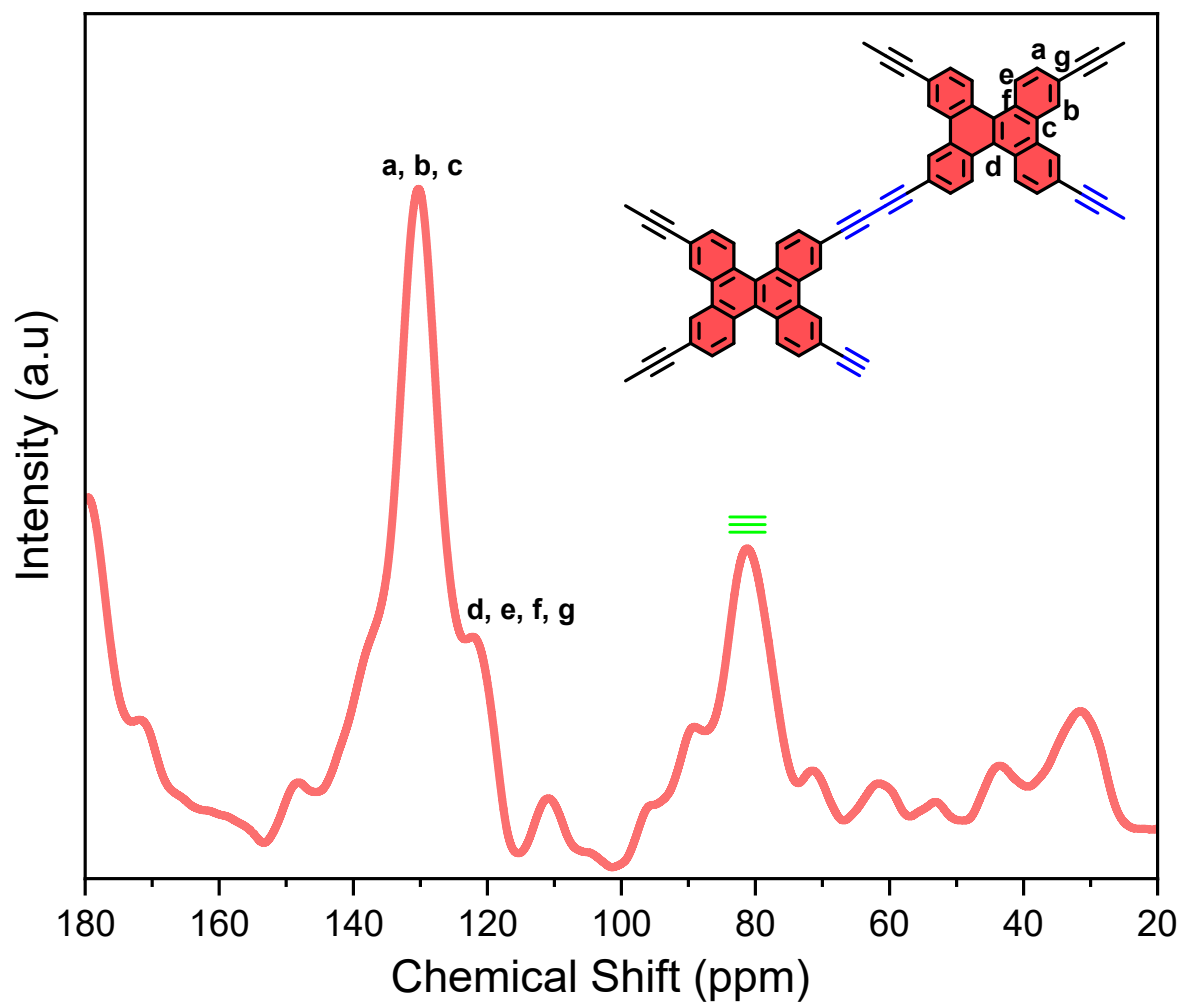


Figure S7. Solid state ^{13}C NMR spectrum of TPE-Diyne CMP.



Fig

re S8. Solid state ^{13}C NMR spectrum of TBN-Diyne CMP.

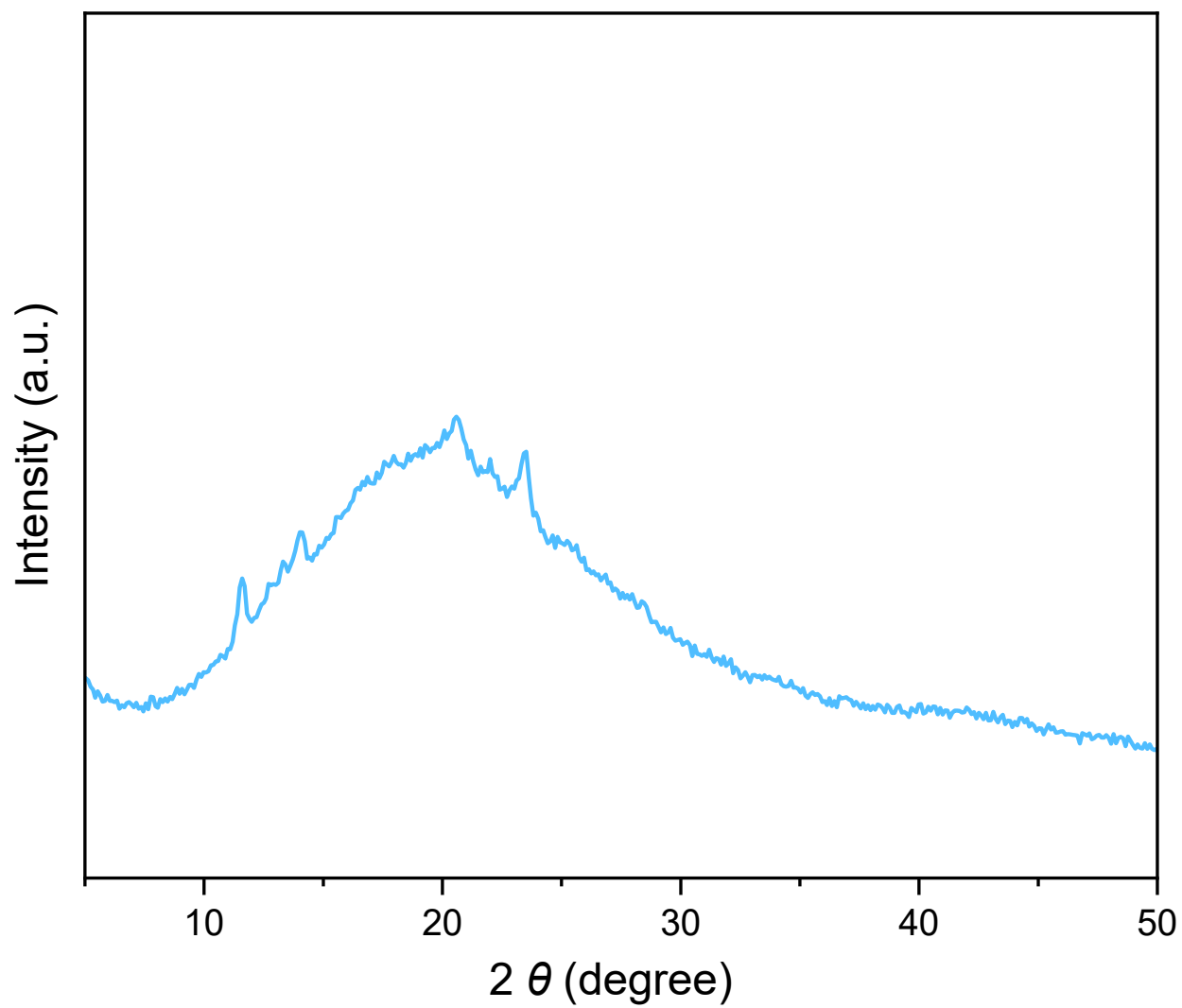


Figure S9. XRD profile of TPE-Diyne CMP.

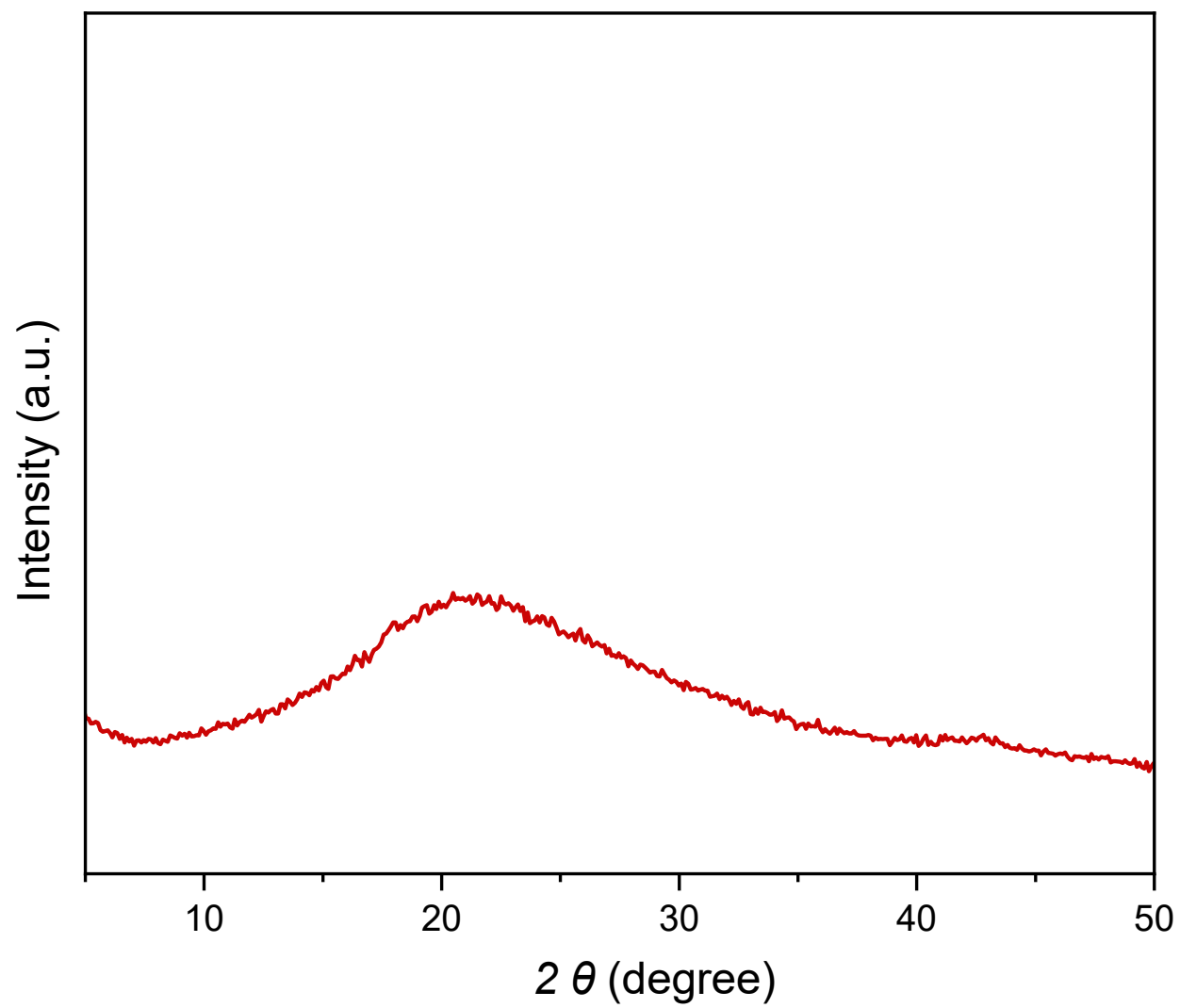


Figure S10. XRD profile of TBN-Diyne CMP.

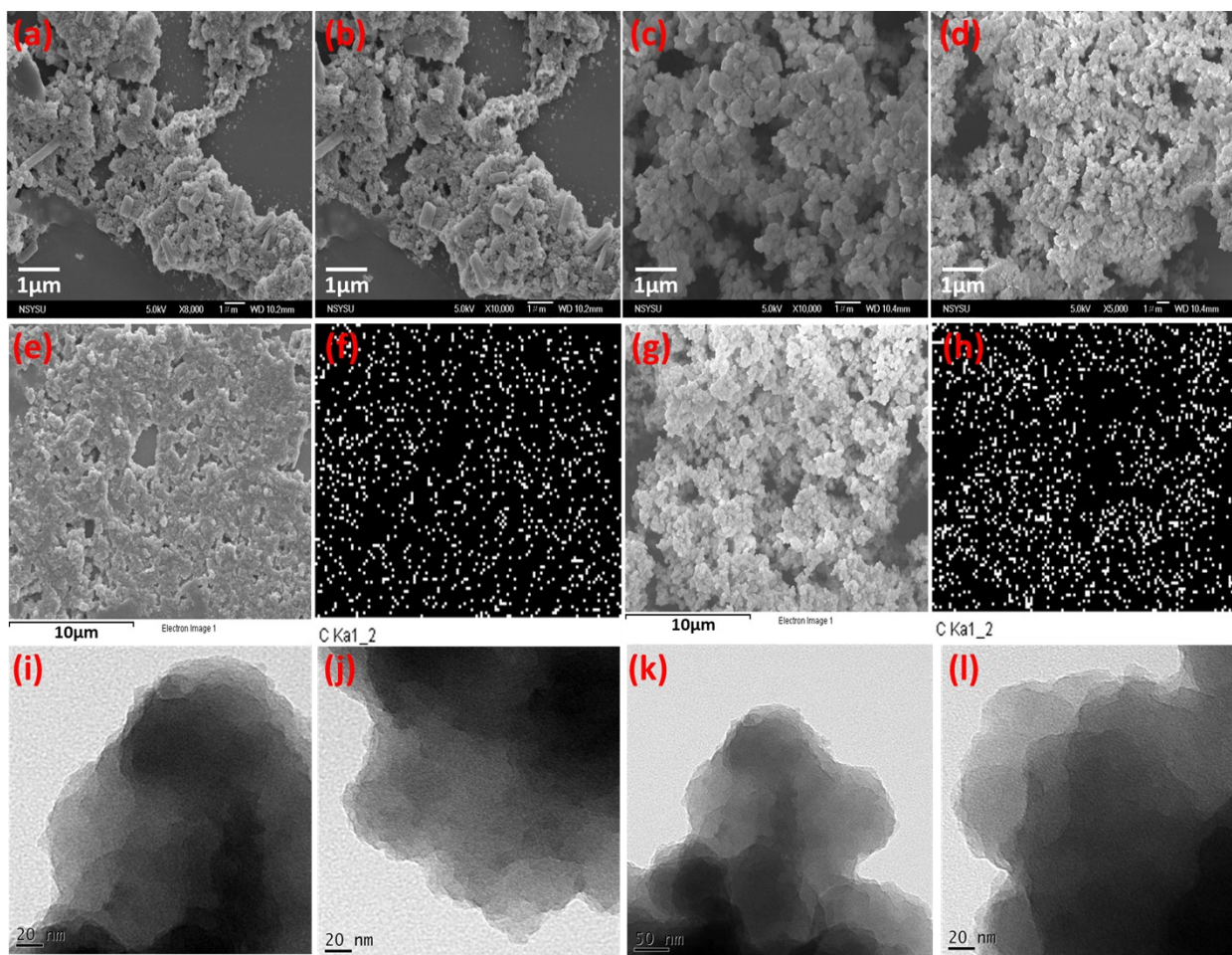


Figure S11. (a-d) SEM, (e-h) SEM-EDS mapping, and (i-l) TEM images of (a, b, e, f, i, j) TPE-Diyne CMP and (c, d, g, h, k, l) TBN-Diyne CMP.